Neural Modified Super-Twisting Filed-Oriented Approach of Asynchronous Machine Drives

Habib Benbouhenni*‡, Dalal Zellouma**

* LAAS laboratory, National Polytechnic School of Oran- Maurice Audin, BP 1523 Oran El M'naouer, Algeria

** LEVRES Laboratory, Department of Electrical engineering, University of El Oued, P.O. Box 789, El-Oued, Algeria

(habib.benbouhenni@enp-oran.dz, dalalzellouma@gmail.com)

‡Corresponding Author; Habib Benbouhenni, BP 1523 Oran El M'naouer, Tel:+213 663956329,

habib.benbouhenni@enp-oran.dz

Received: 22.03.2025 Accepted:31.03.2025

Abstract- This paper proposes a novel field-oriented control (FOC) strategy with a neural-modified super-twisting algorithm (NMSTA) controller for a category of nonlinear systems. This designed control is used to adjust the speed and torque of the asynchronous machine (AM) to enhance the dynamic response, tracking error, and robustness. Also, to reduce the torque, current, and flux undulations of the AM. The FOC-NMSTA technique of the AM has been simulated in MATLAB and compared with the FOC technique. The comparative results obtained under different operating conditions prove the superior performance and robustness of this proposed new intelligent nonlinear technique (FOC-NMSTA). In all four tests, the current harmonic distortion value was improved by 85.96% and 77.91%. Also, the FOC-NMSTA provided a better ripple value of flux than the FOC, where the reduction rates in all tests were 87.76% and 86%. Torque overshoot in all tests was also reduced compared to the FOC with percentages estimated at 41.02% and 44%. These relatively high percentages indicate the extent of FOC-NMSTA's competence and ability to improve the features of the control system.

Keywords Field-oriented control, neural modified super-twisting algorithm, dynamic responses, and asynchronous machine.

1. Introduction

Authors There are many electric machines (EMs), as they are used in many diverse scopes, such as traction. Recently, it has been used in the area of renewable energies to produce electrical power and overcome the problem of global warming. These electrical machines can be classified according to the type of current into alternating current electrical machines and direct current EMs. Accordingly, there are synchronous machines (SMs) [1], asynchronous machines (AMs) [2], stepper electric machines [3], direct current EMs [4], brushless electric machines [5], universal electric machines [6], reluctance electric machines [7], and linear EMs [8]. These electrical machines differ from each other in terms of cost, maintenance, working principle, efficiency, ease of control, and regular maintenance.

Traditionally, AMs are considered one of the most famous and widespread in various fields because of their many advantages. These machines are characterized by high robustness, easy to control, inexpensive, and do not require regular maintenance, which makes them among the most suitable and reliable solutions [9]. AMs are of many types, such as linear AMs [10], doubly-fed AMs [11], and squired cage AMs [12].

As is known, most of the energy consumption resulting from industrial and commercial applications in the world is responsible for AMs due to their advantages such as high efficiency, robustness, and practicality. However, the occurrence of unexpected malfunctions may affect their proper operation, leading to unnecessary malfunctions with economic repercussions. For this reason, developing control approaches that ensure the proper operation of these EMs is very important. These control approaches are varied, highlighting that many nonlinear, linear, hybrid, or intelligent approaches have recently proposed in the literature. In the work [13], the author used field-oriented control (FOC) to control the 3-phase AM, where a proportional-integral (PI) regulator was used to control the feature quantities. Also, the pulse width modulation (PWM) control was used to run the AM inverter. This control was realized in MATLAB using

numerous tests. This control has a fast dynamic response (DR) with undulations at the torque and current levels, which is a negative matter that limits its spread in the control area. Sliding mode control (SMC) is a nonlinear approach that was proposed in the paper [14] to control the AM, where the use of this control depends on knowing the mathematical model (MM) of the AM. In addition to knowing the MM of the AM, this control depends on estimating both flux and torque, which makes it affected in the event of a fault in the AM. However, the results showed the higher efficiency of this control compared to the FOC, which is positive.

As is known, several nonlinearity approaches have been applied to AMs, such as backstepping control (BC) [15], adaptive control [16], super-twisting control (STA) [17], and so on. Therefore, the STA is considered one of the most prominent nonlinear techniques, robust, simple, and easy to implement [18]. Also, this approach has a small number of gains which makes it easy to adjust compared to many other techniques such as BC. Using the STA does not require information on the MM of the EM under study, which makes it one of the most appropriate and reliable solutions for regulating motors [19]. In [20], the author conducted a comparative study between the STA and synergetic control (SC) to find out which control can improve the features of a power system based on the asynchronous generator (AG). First, the disadvantages and advantages of each order were highlighted, stating the MM for each approach. Second, the necessary equations were given to be able to test the control powers of this approach. Third, a simulation of the approaches was completed using a 1.5 MW generator, where the necessary results were extracted. The results obtained show the advantage of the SC over the STA in terms of energy response time (RT) and stream total harmonic distortion (THD). Accordingly, this completed work shows that the STA has drawbacks that distinguish it compared to other approaches.

In the area of control, several techniques have been proposed to defeat the cons of the STA, such as the use of genetic algorithm (GA) [21], fuzzy logic (FL) [22], fractional calculus [23], neural networks (NNs) [24], interval type-2 FL-NN technique [25], particle swarm optimization [26], integral action approach [27], SC [28], and NN-FL technique [29]. In the work [30], the author designed a new STA named simplified STA technique to replace the traditional STA technique. This designed approach has been applied to an AG to get better fineness of power and current. The features of the simplified STA are that it is easy to realize, uncomplicated, simple, and has few gains compared to the STA. Results show that the simplified STA has better numerical results than the PI approach. But, despite its performance, this approach has cons that lie in its reliance on estimating distinct quantities and being affected by changes in system parameters, and this is demonstrated by the robustness test, where degradation of the performance parameters (ripple, overshoot, current THD, and steady-state error (SSE)) is observed. In the work [31], the author used super-twisting integral SMC (ST-ISMC) as a suitable solution to replace the traditional approach, where nonlinear extended state observer (ESO) was used to increase efficiency and stability. This designed control differs from other approaches in terms of the number of gains, competence, working principle, and reliance on the MM of the system. The behavior of the designed control was compared with the PI approach, and the results showed the high efficiency of this control in getting better the features of the permanent magnet SM compared to the PI approach. The cons of this approach lie in the complexity due to its use of ESO and the presence of an important number of gains, which makes it hard to adjust the DR and the use of intelligent algorithms in calculating gains values. Another improved approach for STA was proposed in [32] based on the use of a finite time ESO (FTESO), where this approach was proposed for quadcopter UAV formation. Compared to the STA, this designed control appears more robust and efficient, having remarkable competence and being very effective in getting better the features of the studied EM, and this is demonstrated by the results. However, this designed technique has drawbacks, which lie in the high level of complexity resulting from the use of FTESO and the existence of an important number of gains. Also, it is observed that there is a negative effect on the performance when changing the system parameters, which is undesirable.

The dual STA technique is the solution that was adopted in the work [33] to defeat the defects of the STA of AG, where two different STA controllers were used in parallel for this purpose. This dual STA technique was used to control powers and determine voltage reference values, but it should be mentioned that its use led to an increase in the level of difficulty, the number of gains, the costs, and the degree of difficulty in the experimental implementation of the system. But despite these drawbacks, the results in all tests showed that the dual STA technique has high efficiency and great robustness, and this is demonstrated by the performance indicators (energy undulations, stream's THD, overshoot, and SSE) that are better compared to STA. Third-order continuous STA was designed in [34] as an alternative to the STA approach, where this designed regulator was used to get better the energy quality produced by the 5-phase permanent magnet synchronous wind generator. The designed controller differs from the conventional controller in terms of the number of gains, performance, durability, and ease of realization. The outputs of the designed approach are reference voltage values (RVVs), and these values were used to create functioning pulses for the machine inverter. MATLAB was used to realize this designed control and compare it with the PI control in terms of minimizing energy undulations and current THD. Results demonstrate the high efficiency of the third-order continuous STA compared to the PI control in terms of getting better the features of the studied EM. This designed control has drawbacks that lie in the presence of a significant number of gains and a maximal level of intricacy than the PI control, which makes it expensive and undesirable.

One of the smart approaches that is considered the most widespread and widely used in the area of control is NNs. This approach has been used to better the features of several approaches such as direct torque control (DTC) [35], direct power control (DPC) [36], and FOC technique [37]. Using this approach led to an increase in the characteristics of control techniques, such as robustness and competence, this is a positive thing that shows the extent of the ability of NNs to enhance competence. The strength of NNs lies in the fact that

their use does not require information about the MM of the EM, which gives them high competence in the event of a fault in the studied system. Also, NNs are characterized by high accuracy, which makes them give superior results compared to other strategies. In the work [38], the author used NNs to improve the characteristics of the space vector modulation (SVM), where experimental work was used to confirm the extent of the ability and efficacy of NNs in improving the features of the SVM. Compared to both PWM and SVM, the use of NNs in the SVM led to getting better current THD and improved controllability of the fundamental signal (50Hz). Fractional calculus and NN were combined to find a regulator with high stability and the ability to ameliorate the AG features [39]. This proposed regulator is categorized by simplicity, few gains, and ease of realization, which makes it one of the most important solutions that can be relied upon in the future. Also, its application does not require information on the MM of the equipment under study, which gives it an advantage in the event of a fault in the equipment. The results show that the fractional-order NN has a distinctive efficiency compared to the PI control, and this is shown by the reduction ratios determined for the main performance indicators. The cons of this approach lie in its reliance on energy estimation, which makes it slightly affected in the robustness test by changing system parameters. In [40], NNs were used to improve the features of the PI-DPC. Neural PI control is a modification of PI control, which is categorized by simplicity, small number of gains, inexpensive, and easy to realize. The use of NNs led to better characteristics compared to the PI control, and this is demonstrated by the results obtained in all tests. In the work [41], FL and NN were combined to control the powers of an AG. The designed control is simple, uncomplicated, and easy to realize. This approach relies heavily on the designer's experience, as it does not need to know the MM of the EM under study. Experimental results show the high advantage of this approach in minimizing stream and torque undulations. Also, this suggested control has a fast DR, which makes it suitable in the future for regulating equipment. Despite the high performance of this control, the experimental results show that current and torque undulations remain present.

In [42], NNs were used to ameliorate DPC features using the SC-STA strategy (a combination of the synergetic control with super-twisting control). So, the NN-SC-STA is a modification of the SC-STA, which is categorized by simplicity, small number of gains, inexpensive, and easy to apply. The use of NNs led to getting better features of the NN-SC-STA compared to the SC-STA, and this is demonstrated by the results obtained in all tests. This approach was implemented using MATLAB and compared with the PI and other scientific works, and the numerical results showed the performance of this control in improving the currents THD and power quality. The cons of this approach lie in the use of energy estimation, which makes it give unsatisfactory results in the event of a fault in the EM, as it is observed that the value of the stream/power undulations, and the value of THD, overshoot, and SSE are higher in the robustness test compared to the reference tracking test, which is undesirable. One of the applications of NNs in the area of control is the work done in [43], where this control was used to get better features of the modified SMC of the AGs. The NN approach was relied upon for its high competence and ability to improve the features of approaches, as it was used to replace the function sign(u) of modified SMC. The resulting control is simple, inexpensive, does not require information on the MM of the equipment, has a small number of gains, and can easily be accomplished experimentally. The results showed the high competence of the suggested control in getting better the features of the studied system and this is demonstrated by the numerical values of undulations, overshoot, RT, and SSE compared to the PI control and some papers. In the work [44], NNs were used to defeat the cons of the DTC of dual AMs, where these two machines are fed by only one inverter. The designed system is simple, inexpensive, and of great significance in the industrial field. A NN was used to compensate the lookup table for the DTC and create the pulses needed to work the inverter. This suggested control was verified in MATLAB, with results compared to the DTC. Results in all tests show that the use of NNs led to a minimization in current undulations and a significant increase in the DTC robustness of dual AMs. Also, the stream THD, SSE, and overshoot are reduced compared to DTC.

The analysis of the works mentioned above, shows that the integration of NN and STA can generate a new control with high characteristics. This proposed work presents a solution characterized by great effectiveness and distinctive competence, as it is designed to use a modified STA based on NN to improve the features of the AM-based control system. So, the neural modified STA (NMSTA) is the main contribution of this study, as this suggested controller differs from the controllers mentioned above in terms of efficiency, robustness, number of gains, degree of complexity, simplicity, and ease of realization. This suggested controller is used to control AM operation using FOC. So, the FOC-NMSTA is the second major contribution of this paper. The FOC-NMSTA is a modification of the FOC-PI, as it is based on the use of the PWM to create the pulses needed to activate the AM inverter. High robustness, outstanding competence, and great effectiveness in minimizing torque and current undulations are among the biggest positives of this designed FOC-NMSTA. MATLAB was used to realize this FOC-NMSTA strategy, where numerous tests were implemented to study the competence and compare the results with the FOC-PI. By implementing the FOC-NMSTA, the following objectives were achieved:

- Significantly improvement in current THD
- Improved torque and flux quality compared to the PI-FOC-PI approach
- Significantly increased control system durability
- Reducing overshoot and SSE values compared to the FOC-PI approach
- Improving AM's FOC features

The paper has six sections. The AM model is described in Section 2. In Section 3, a mathematical representation of the NMSTA technique is presented along with the advantages and disadvantages of this designed controller. The FOC-NMSTA approach of AM is presented in Section 4. The comparison simulation outcomes for an AM drive are displayed in Section

5. The last section contains the conclusions obtained from this completed study.

2. AM Model

In this work, a squirrel cage type AM is used, considered one of the most famous types in the industrial area due to its ease of control, high robustness, and low repairs. Also, this type of motor has a low cost which makes it suitable for any industrial application [45]. The rotor of this motor is in the shape of a squirrel cage, which makes it more rigid than any other type [46, 47]. The Park transform is the most widely used method to provide an MM for any electrical machine, as this theory is used to give the mathematical equations that express the operation of the machine. Therefore, using the Park transformation allows the MM to be given for each part of the machine, as the machine has an electrical part and a mechanical part.

According to the work [48], the machine voltage is expressed by Equation (1).

$$\begin{cases} V_{ds} = R_s I_{ds} + \frac{d}{dt}\psi_{ds} - \omega\,\psi_{qs} \\ V_{qs} = R_s I_{qs} + \frac{d}{dt}\psi_{qs} + \omega\psi_{ds} \\ 0 = R_r I_{dr} + \frac{d}{dt}\psi_{dr} - (\omega - \omega_r)\,\psi_{qr} \\ 0 = R_r I_{qr} + \frac{d}{dt}\psi_{qr} + (\omega - \omega_r)\,\psi_{dr} \end{cases} \quad (1)$$

Where, *Rr* and *Rs* are the rotor and stator resistances; ψ_{ds}, ψ_{qs} , ψ_{dr}, and ψ_{qr} are the rotor and stator dq-axis fluxes; V_{ds}, V_{qs}, V_{dr}, and V_{qr} are the stator and rotor dq-axis voltage; ω and ω_r are the rotation speed and reference rotation speed. Equation (2) considers the flux of the machine, where this flux is related to the current. Therefore, to know the change in flux, the change in current must be known.

$$\begin{cases} \psi_{ds} = L_s I_{ds} + M I_{dr} \\ \psi_{qs} = L_s I_{qs} + M I_{qr} \\ \psi_{dr} = L_r I_{dr} + M I_{ds} \\ 0 = L_r I_{qr} + M I_{qs} \end{cases} \quad (2)$$

Where, L_s and L_r are defined as stator and rotor self-inductance, respectively [47, 48].

$$\begin{cases} V_{ds} = R_s I_{ds} + L_s\sigma\frac{d}{dt}I_{ds} + \frac{M}{L_r}\frac{d}{dt}\psi_{dr} - \omega_s\, L_s\sigma I_{qs} \\ V_{qs} = R_s I_{qs} + L_s\sigma\frac{d}{dt}I_{qs} + \frac{M}{L_r}\frac{d}{dt}\psi_{dr} + \omega_s\, L_s\sigma I_{ds} \end{cases} \quad (3)$$

The evolution of the speed change is shown in Equation (4), where the rotation speed change is related to the difference between the machine torque and the load torque. Therefore, this equation is responsible for the operation of the AM, motor, or generator. This equation expresses the mechanical part of the AM.

$$\frac{d}{dt}\Omega_r = \frac{1}{j}(T_e - T_L - f_r\Omega_r) \quad (4)$$

Where, Ω is stated as the mechanical rotor speed, T_L is the mechanical torque, and T_e is the torque.

Equation (5) expresses the torque of the AM, where this torque is related to the stream and flux values. In order to change the torque, it is enough to change the current.

$$T_e = \frac{3M}{2L_r}p(\psi_{dr}I_{qs} - \psi_{qr}I_{ds}) \quad (5)$$

3. Proposed Intelligent Nonlinear Approach

In this part, a novel regulator is proposed that is based on the combination of two different approaches: NNs and the MSTA technique. To understand the characteristics of the designed control, the MM of the studied system, and the pros and cons, the MSTA technique must be addressed first.

3.1 MSTA Technique

The MSTA is a change and amendment of the STA. The latter is a nonlinear approach that was proposed by Levant in 1993 to replace the SMC approach [49]. The STA approach has been used to improve the effectiveness, performance, and robustness of many techniques such as the DTC strategy [50] and the DPC approach [51]. According to the work done in [52], the STA can be easily applied to complex systems, which gives it an advantage over numerous other controls such as BC approaches. The authors see in the two works [53, 54] that the STA is a development and modification of the PI controller and a simplification of the use of second-order SMC. However, the use of the STA is accompanied by a set of cons that limit its spread, as in the event of a fault in the EM, this control provides unsatisfactory results, which is undesirable. Numerous solutions were designed to defeat the cons and their shortcomings, where the most prominent solutions were the use of smart approaches and nonlinear approaches.

The MSTA is a new idea to improve the ability, efficiency, competence, and robustness of the STA. This approach is a change and adjustment of the STA, where the MSTA can be expressed using Equation (6). The MSTA is robust, simple, and easy to realize. Also, having few gains makes it easy to adjust.

$$u(t) = u_1\,(t) + u_2\,(t) + u_3\,(t) \quad (6)$$

With:

$$u_1\,(t) = K_1\sqrt{|S|}Sign(S) \quad (7)$$

$$u_2\,(t) = K_2\int Sign(S)dt \quad (8)$$

$$u_3\,(t) = S \quad (9)$$

Where, K_1, K_2, and K_3 are the positive gains. By means of the values of these gains the DR can be regulated and changed. *S* is the sliding surface.

The mathematical form in Equation (6) can be illustrated by Figure 1.

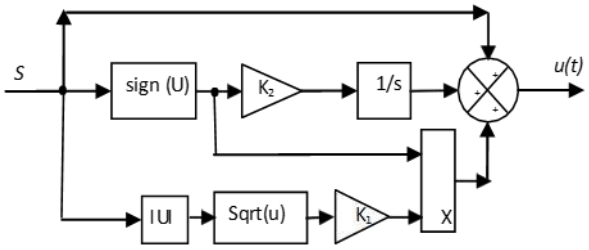

Fig. 1. The MSTA controller.

The use of the sign(U) function in the MSTA approach creates several problems and disadvantages and limits the spread of this control in the future. Therefore, to increase the efficiency and robustness of this control, it is designed to compensate for the sign(U) using an NN controller, and in the next subsection, sufficient information is given about this accomplished change.

3.2 Neural MSTA Strategy

The control designed in this subsection is a change and development of the MSTA, where NNs were used as a solution to increase competence and robustness. Neural algorithms have been adopted as a solution due to their ease of use, high robustness, and imperviousness to internal or external factors within the system, enabling high performance. Furthermore, this algorithm boasts a rapid dynamic response, allowing its use in systems to significantly improve response time. Furthermore, accuracy is a key feature of neural algorithms, making them a reliable solution in the field of control.

The neural MSMC approach combines a neural algorithm with an MSTA controller to produce a new approach with high robustness and strong operational performance. Based on Equation (6), the mathematical model of the proposed approach is derived, where a neural algorithm is used in place of the sign(U) function of the MSTA. This improves the performance and efficiency of the MSTA controller. The MM of the neural MSMC approach is represented by Equation (10).

$$y(t) = K_1 \sqrt{|S|} \times Neural(S) + S + K_2 \int Neural(S)dt \quad (10)$$

Equation (10) can be represented by Figure 2 to further clarify the proposed NMSTA technique, where robustness, ease of completion, simplicity, small number of gains, and high performance are among the most important features of this proposed NMSTA technique.

The NMSTA technique's gain values can be calculated using intelligent strategies such as genetic algorithms or Grey Wolf optimization. Additionally, experimentation and simulation can be used to calculate these gain values. This method does not require complex programming or time, as is the approach used in this paper.

In terms of computational complexity, the NMSTA technique does not require complex calculations, as it can be easily applied to complex systems without needing to know their mathematical models. This feature makes the proposed approach a promising solution in the field of control.

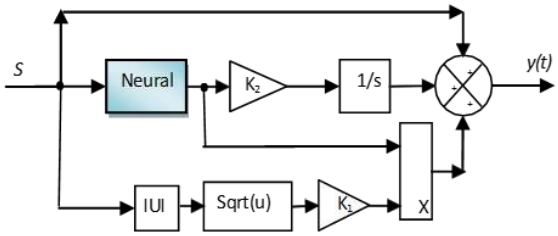

Fig. 2. The NMSTA controller.

The type of NN approach used in this study is a trainable cascade backpropagation network, and newcf is the function used in MATLAB to call it. The neural controller used has only one input and one output, and the gradient descent with momentum and adaptive LR (ALR) was used to achieve it. The parameters of the ALR used are represented in Table 1.

Table 1. ALR parameters

ALR parameters	Values
Trainparam.show	50
Functions of activation	Tensing, Purling, and Traincgb
Trainparam.lr	0.01
Coeff of acceleration of convergence (mc)	0.8
Trainparam.goal	0
Number of neurons in the hidden layer.	10
Trainparam.eposh	1000
Number of hidden layers	1
Trainparam.mu	0.08

Figure 3 shows the graphical properties of the NN used to improve the features of the MSTA approach. Figure 3a shows the validation checks, gradient, and step size. From Figure 3a the best value for gradient was 0.19623 at epoch 50. Also, the best value for validation checks was 0 at epoch 50. The best value for step size is 0.0072211 in the case of epoch 50. In Figure 3b the training performance of the NN technique is shown, where the best training performance is 0.0033822, at epoch 50. Figure 3c shows the target of the NN approach, as from this figure the output value can be known. The output value is the multiplied two numbers (target and 1) plus 0.021. This figure expresses the degree to which the output follows the input, as it is noted that training: R=1, which indicates that the NN controller has a high-performance response.

In Figure 4 the internal organization of the NN technique is given, as it consists of two layers. In Figure 4b and 4c, the internal structure of each layer is given.

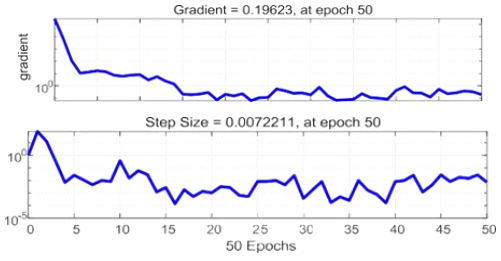

(a)

(b)

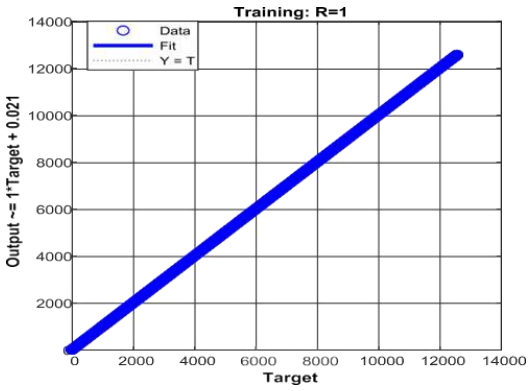

(c)

Fig. 3. Graphical properties of the NN used: a) Gradient, validation checks, and step size, b) Training, and c) Target.

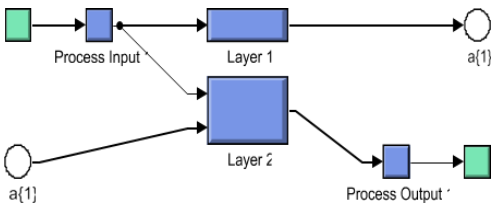

(a) NN controller

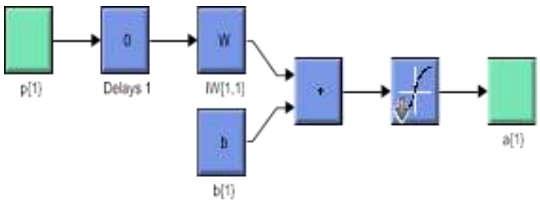

(b) Layer 1

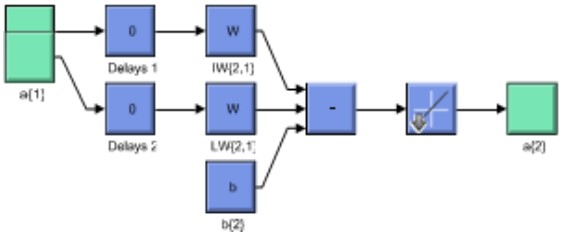

(c) Layer 2

Fig. 4. Structure interne of NN controller.

4. Designed AM Control

The approach designed in this part is based on the use of the FOC, as the regulator proposed in the previous part is used for this purpose. The FOC-NMSTA aims to ameliorate the features of the FOC and significantly increase the machine's performance. Also, to ameliorate the current quality and thus minimize the peak torque and flux undulations. So, to understand the working principle of FOC-NMSTA, the FOC-PI MM must be presented first because FOC-NMSTA is a development of FOC-PI.

4.1. Conventional FOC Method

Conventionally, the FOC is considered one of the most prominent nonlinear controls that appeared in the last century for controlling machines, especially AMs, as it has a fast DR. This control depends on the use of a PI in the internal loops and on the use of the PWM to create operating pulses for the AM inverter.

The FOC is based on the principle shown in Figure 5, where this principle lies in aligning the rotor flux vector with the d-axis of the rotational reference frame.

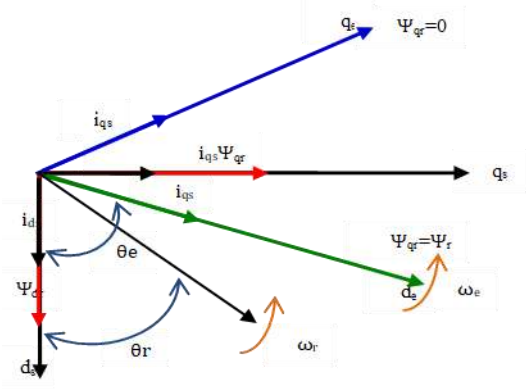

Fig. 5. Principle of FOC technique.

Using the work done in [55], where ψ_{qr}=0 is made, the flux can be written according to Equation (11).

$$\begin{cases} \psi_{dr} = \psi_r \\ \psi_{qr} = 0 \end{cases} \tag{11}$$

To apply the FOC approach to an AM machine, the MM for this machine must be given according to the Park transformation using dq axes. Using the Park transformation, the machine can be represented by a set of nonlinear differential equations with two magnetic and two electrical coordinates, where the stator voltages represent the two mechanical inputs to the system. According to the two works [56, 57], AM can be described by the following equations:

$$\begin{cases} \frac{d}{dt}I_{ds} = -\left(\frac{1}{\sigma T_s}+\frac{M^2}{\delta L_r T_r}\right)I_{ds} + \omega_s I_{qs} + \frac{M}{\delta L_r T_r}\psi_{dr} + \delta V_{ds} \\ \frac{d}{dt}I_{qs} = -\left(\frac{1}{\sigma T_s}+\frac{M^2}{\delta L_r T_r}\right)I_{qs} - \omega_s I_{ds} - \frac{M}{\delta L_r}\omega\psi_{dr} + \delta V_{qs} \\ \frac{d}{dt}\psi_{dr} = \frac{M}{T_r}I_{ds} - \frac{1}{T_r}\psi_{dr} \\ \frac{d}{dt}\Omega = \frac{3M}{2JL_r}p\psi_{qr}I_{qs} - \frac{T_L}{J} - \frac{f}{J}\Omega \end{cases} \quad (12)$$

In the d-q axes, the MM is defined by two equations:

$$\begin{cases} \dot{x} = \mathrm{A[x]} + \mathrm{B[u]} \\ y = C[x] \end{cases} \quad (13)$$

With: $\dot{x} = [I_{ds}\ I_{qs}\ \psi_{dr}\ \psi_{qr}]$; $\mathrm{u} = [V_{ds}\ V_{qs}]$; $\mathrm{y} = [I_{ds}\ I_{qs}]$

The Equations (14) and (15) represent the MM of the system in the form of matrices.

$$A = \begin{bmatrix} -\left(\frac{1}{\sigma T_s}+\frac{M^2}{\delta L_r T_r}\right) & 0 & \frac{M}{\delta L_r T_r} & \frac{M}{\delta L_r} \\ 0 & -\left(\frac{1}{\sigma T_s}+\frac{M^2}{\delta L_r T_r}\right) & -\frac{M}{\delta L_r} & \frac{M}{\delta L_r T_r} \\ \frac{M}{T_r} & 0 & -\frac{1}{T_r} & 0 \\ 0 & \frac{M}{T_r} & 0 & -\frac{1}{T_r} \end{bmatrix}; \mathrm{B} = \begin{bmatrix} \delta & 0 \\ 0 & \delta \\ 0 & 0 \\ 0 & 0 \end{bmatrix} \quad (14)$$

$$C = \begin{bmatrix} 1 & 0 & 0 & 0 \\ 0 & 1 & 0 & 0 \end{bmatrix} \quad (15)$$

With: $T_s = \frac{L_S}{R_S}$; $T_r = \frac{L_r}{R_r}$; $\delta = \frac{1}{\sigma L_s}$; $\sigma = \frac{M}{L_S L_r}$

Figure 6 shows the FOC-PI for the AM motor, as it is noted that it uses four PI-type controllers, and the PWM approach is used to control the process of the AM inverter. This approach relies on the use of a speed pickup to calculate the speed error, which makes it an experimentally expensive approach. Also, it is noted that this approach does not use estimation of both flux and torque, which makes it simple and uncomplicated.

The reliance of this control on PI-type controllers causes undulations at the level of both torque and current in the event of a fault in the AM. Also, this control offers a high current THD compared to some existing controls.

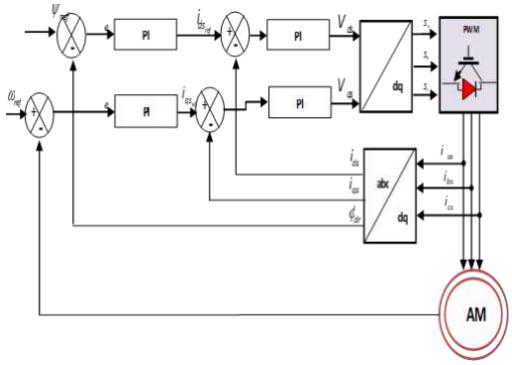

Fig. 6. The FOC-PI technique of the AM.

In the next subsection, the proposed solution is discussed to defeat the cons and drawbacks of the FOC of AM.

4.2. Proposed FOC-NMSTA Approach

The FOC-NMSTA is a new proposal that was designed for the first time in this paper to control the AM rotation speed, as it is considered a hybrid approach. The proposed approach relies on integrating both NNs and the MSTA to control the characteristic magnitudes. This designed technique aims to decrease the flux undulations and torque of the AM. This designed technique is an adjustment and development of the FOC-PI, where the PI controllers were replaced with NMSTA-type controllers. One of the most prominent features of this designed FOC-NMSTA is its flexibility and not being affected by changing AM parameters, which makes it give good results in terms of current and torque fineness.

Figure 7 shows the proposed FOC-NMSTA approach for controlling machine torque and flow, where four NMSTA controllers are used for this purpose. This suggested approach relies on the use of internal loops (current loops), wherein in the first loop the reference values of the current are determined based on the velocity and flux errors. In the first episode, an NMSTA controller is used. The second loop uses an NMSTA control, where the RVVs are determined based on the current reference values. These VRVs are used to run the AM inverter, and the PWM is used for this purpose.

This designed FOC-NMSTA technique is described by high effectiveness, outstanding competence, and robustness in minimizing torque and current fluctuations more than the FOC-PI. In Table 2, the differences and similarities between the designed and FOC-PI approaches are given in terms of number of gains, ease of completion, degree of complexity, etc.

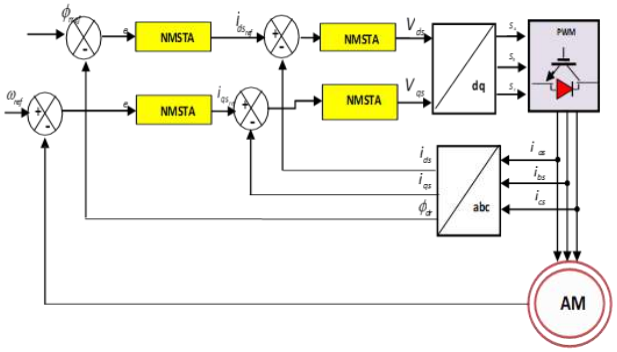

Fig 7. The FOC-NMSTA of the AM drive.

Table 2. Comparative analysis of the conventional and developed FOC approaches

	FOC-PI	**FOC-NMSTA**
Dynamic response	Slow	Fast
Modulation strategy	PWM	PWM
Controller	PI	NMSTA
Block of estimation	Yes	Yes
Estimation of torque and flux	No	No
Robustness	Low	High
Torque ripple	High	Low
Simplicity	Simple	Simple
Current THD value	High	Low
Implementation	Easy	Easy
Applied to multi-phase generator	Easily	Easily
Flux quality	Low	High
Number of controllers used	Four	Four
Current quality	Low	High
Completion cost	Not expensive	Not expensive

To prove the stability of the FOC-NMSTA, Lyapunov's theory or the Bode curve can be used for this purpose. Therefore, using the Bode curve to prove the stability of the approach is considered one of the easiest methods, as it is considered a graphical method that does not require complex calculations. MATLAB can be used to extract the Bode curve, as a curve is extracted for both phase and magnitude. Using these two curves, the stability of the FOC-NMSTA can be confirmed. Figure 8 represents the frequency curves using the Bode technique for both the FOC-PI and FOC-NMSTA. From this figure it can be seen that both phase and magnitude values change with angular frequency, as the angular frequency increases, the magnitude value decreases in the case of the two controls. The value of magnitude in the case of the FOC-PI changes from -50 dB to -250 dB, and in the case of the FOC-NMSTA it changes from 25 dB to - 200 dB. Therefore, the value of magnitude in the case of zero frequency was -75 dB and -8 dB for FOC-PI and FOC-NMSTA, respectively. Phase changes in the range from 360° to -360° in the case of FOC-PI, and the case of FOC-NMSTA it changes from 720° to -180°. In the case of zero frequency, the phase value is 180° and 300° for FOC-PI and FOC-NMSA, respectively.

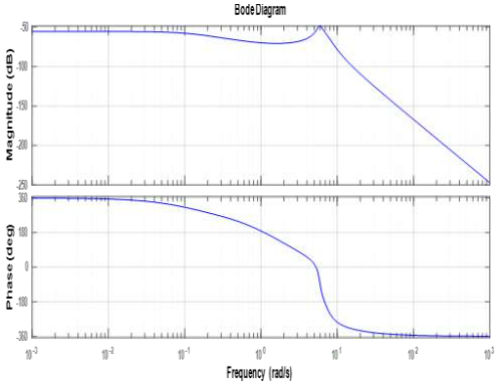

a) FOC-PI

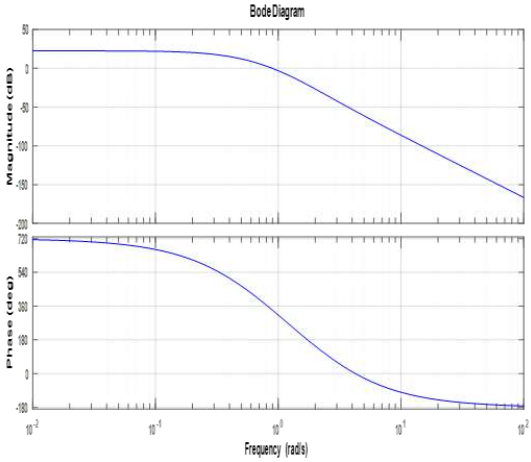

b) FOC- NMSTA

Fig. 8. Bode curve.

In the next section, the proposed FOC-NMSTA strategy will be implemented on a 1.5 kW AM drive, where the competence, robustness, effectiveness, and efficiency of the FOC-NMSTA will be verified compared to the FOC-PI.

5. Results

In this part, the safety, robustness, and competence of the FOC-NMSTA applied to a 1500 W AM are verified, where MATLAB is used for this purpose. The FOC-NMSTA is compared with the FOC-PI using different tests in terms of minimizing flux and torque undulations, current THD, RT, and the value of both overshoot and SSE. The AM parameters are: R_r=4.05 Ω, L_s=0.5763 H, R_s=5.35 Ω, L_r=0.5763 H, L_m=0.556 H, f=0 N.m.s, f_s=50 Hz, J=0.0498 Kg.m2, p=2.

a) Test 1

This test involves tracing the dynamics of the presented FOC-NMSTA at a constant control speed with a load torque changed in time (from 0 to 4 N.m at 1.5 seconds). Figure 9 displays the results that were obtained. Speed and torque follow the reference well for both controls (Figures 9a and 9b), as it is noted that the FOC-NMSTA provided a much better RT to speed than the RT provided by the FOC-PI. Also, the FOC-NMSTA significantly minimized torque undulations compared to the FOC-PI. At the moment 1.5 seconds when the load torque is applied, it is noted that the rotation speed in the FOC-PI has been affected and this appears through its value decreasing for a period of time and then returning to the reference value. However, in the case of the FOC-NMSTA, it is noted that the speed was not affected by the change in the torque value at the time point of 1.5 seconds, which indicates the extent of its ability to improve the features of the AM.

The flux and current are shown in Figures 9c and 9d, respectively. It is noted that the flux of the two approaches follows the reference well, with the FOC-NMSTA having an improvement over the FOC-PI in terms of overshoot value, RT, and undulations. Also, the flux is affected by changing the torque value, as this effect is large in the case of the FOC-PI, but in the FOC-NMSTA this effect does not exist, as the flux value remains well following the reference at the time point of 1.5 s. The current for the two controls is sinusoidal with its value related to the torque (Figure 9d), as it is observed that

when the torque value increases, it is accompanied by an increase in the current value for the two controls. Also, the FOC-NMSTA technique reduced the value of current undulations, as the value of fluctuations was 0.29 A and 0.103 A for both the FOC-PI and FOC-NMSTA, respectively. Therefore, the suggested technique reduced current ripples by an estimated 51.72 % compared to the FOC-PI.

The current THD for the two approaches is represented in Figures 9e and 9f. In the FOC-NMSTA technique, the value of THD was 0.48 % and in the FOC-PI, the value was 3.42 %, which makes the reduction value about 85.96 % for the FOC-PI. Also, it is noted that the two approaches have the same value of the amplitude of the fundamental signal (FS) (50 Hz), where the value of this capacity was 1.471 A.

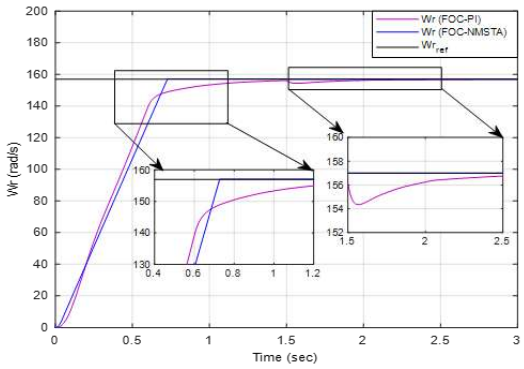

(a) Speed

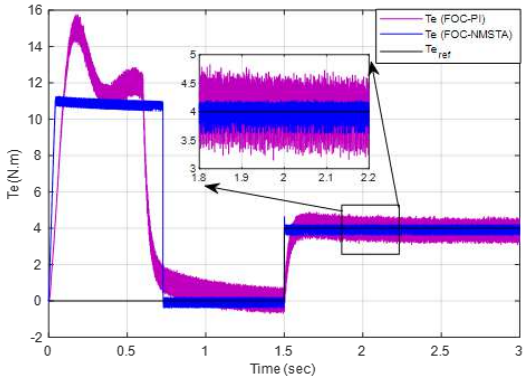

(b) Torque

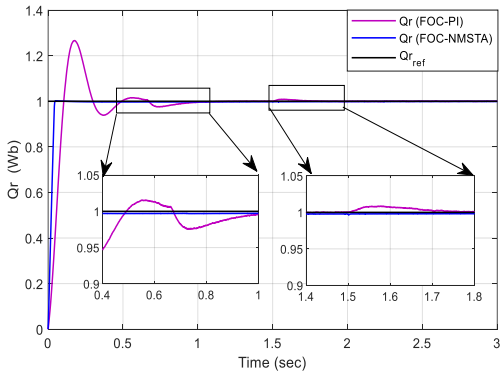

(c) Rotor flux

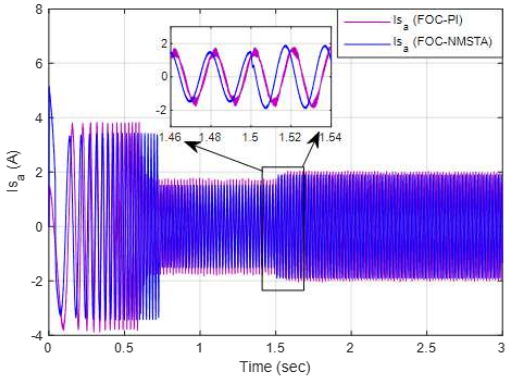

(d) Current

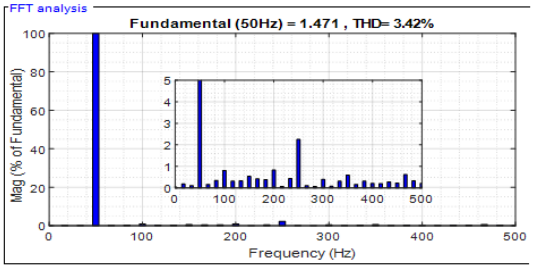

(e) Current THD (FOC)

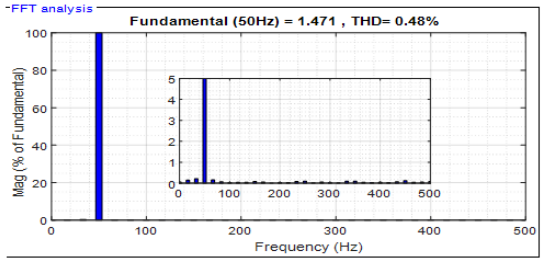

(f) Current THD (FOC-NMSA)

Fig. 9. First test results.

In Table 3, the numerical values obtained from the first test are shown for RT, ripples, undershoot, SSE, and overshoot. The FOC-NMSTA provided better numerical results than the FOC-PI, and this is demonstrated by the determination minimization rates. Accordingly, the FOC-NMSTA reduced the RT to speed, flux, and torque compared to the FOC-PI by ratios estimated at 10.44 %, 40.29 %, and 52.77 %, respectively. Also, the SSE value for velocity and flux was reduced by 30.76 % and 68.91 %, respectively. The FOC-NMSTA reduced torque and flux ripples by rates estimated at 76.19 % and 54.72 %, respectively, compared to the FOC-PI. The FOC-NMSTA reduced speed, torque, and flux overshoot compared to the FOC-PI by rates estimated at 95.99 %, 41.02 %, and 55.55 %, respectively. On the other hand, the undershoot value for speed, flux, and torque was minimized compared to the FOC-PI by ratios estimated at 99.73 %, 90.85 %, and 81.08 %, respectively.

These obtained percentages prove the high efficiency and competence of this control in ameliorating the features of the control system.

Table 3. Statistical results in the Test 1

	Techniques	w_r(rad/sec)	Q_r(Wb)	T_e (N.m)
RT	**FOC-PI**	0.67	0.67	0.36
	FOC-NMSTA	0.06	0.04	0.17
	Ratios (%)	10.44	40.29	52.77
SSE	**FOC-PI**	00.26	00.74	-
	FOC-NMSTA	00.18	00.23	-
	Ratios (%)	30.76	68.91	-
Overshoot	**FOC-PI**	0.63	0.027	0.78
	FOC-NMSTA	0.028	0.012	0.46
	Ratios (%)	95.55	55.55	41.02
Ripples	**FOC-PI**	-	0.0021	0.36
	FOC-NMSTA	-	0.0005	0.163
	Ratios (%)	-	76.19	54.72
Undershoot	**FOC-PI**	1.27	0.07	0.46
	FOC-NMSTA	0.0034	0.0064	0.087
	Ratios (%)	99.73	90.85	81.08

b) Second test: Variation of the reference speed

In this test, the characteristics and competence of the FOC-NMSTA are studied in terms of changing the rotation speed from 80 rad/s to 157 rad/s while applying a load at an instant of 2.2 seconds. The results obtained are represented in Figure 10. Through Figures 10a and 10b, the values of both speed and torque follow the references. The FOC-NMSTA has an advantage in terms of speed RT and torque undulation value compared to the FOC-PI. When the speed is changed at the time point of 1.5 s, it is observed that the torque value is affected by this change, as its value increased to about 11 Nm and 12 Nm for both the FOC-NMSTA and FOC-PI, respectively. This is normal because there is a relationship linking torque and speed (mechanical equation).

The flux and current are represented in Figures 10c and 10d for the two controls, as their values are affected by the change in the torque value and this appears at the time frames of 1.5 and 2.2 seconds. Also, the flux follows the reference well with an overshoot value in the case of using the FOC-PI, but in the case of using the FOC-NMSTA, the overshoot value is nil, which is a positive thing. It is observed in the period from 1.4 to 2.4 seconds that the flux value in the case of using the FOC-NMSTA is not affected by the change in the torque value compared to the FOC-PI that was affected, which is a good thing that proves the strength and robustness of the FOC-NMSTA. Also, the current continues to take a sinusoidal shape with fewer ripples if the FOC-NMSTA is used, as these ripples were 0.42 A and 0.28 A for both the FOC-PI and the FOC-NMSTA, respectively. So the FOC-NMSTA reduced current ripples by an estimated 93.33 % compared to the FOC-PI.

Figures 10e and 10f show the value of both fundamental and current THD of both techniques. So the FOC-NMSTA provided a lower value for THD (0.57 !%) compared to the FOC-PI (3.64 %), as this reduction was estimated at 84.34 %, which shows that the current quality is very high if the FOC-NMSTA is used. Also, it is noted that the FOC-NMSTA has an amplitude of the FS that is relatively lower than the amplitude provided by the FOC-PI, as the value of this amplitude was 1.47 A and 1.464 A for both the FOC-PI and FOC-NMSTA, respectively. Therefore, the value of the amplitude of the FS is the negativity of the FOC-NMSTA in this test.

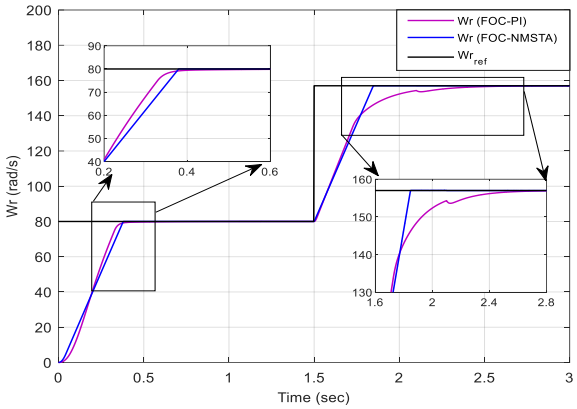

(a) Speed

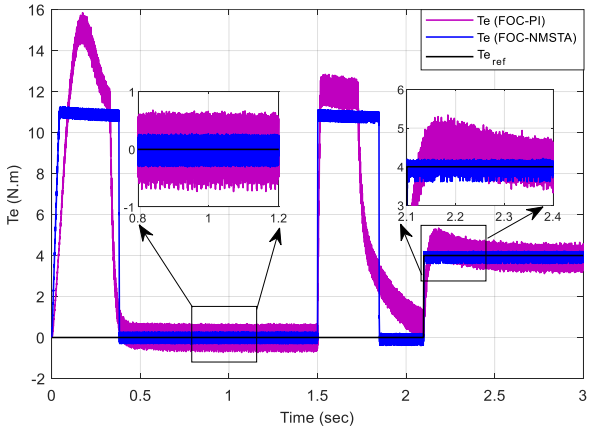

(b) Torque

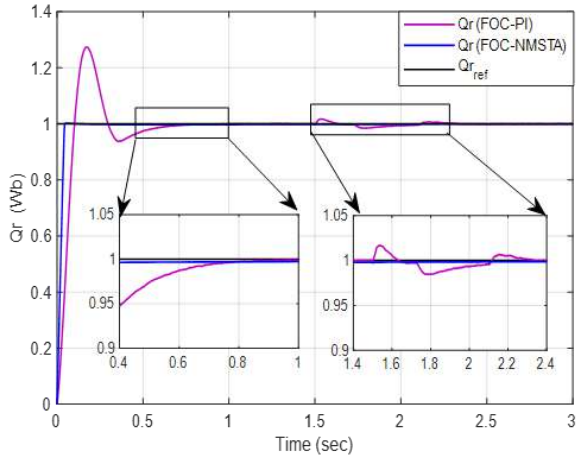

(c) Rotor flux

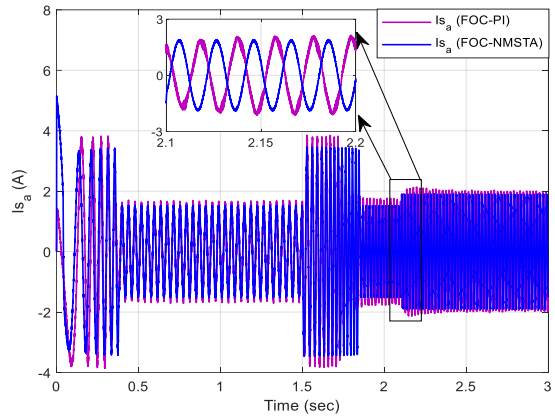

(c) Current

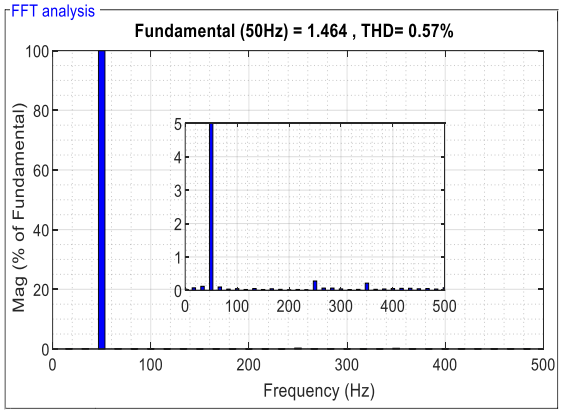

(d) Current THD (FOC-PI)

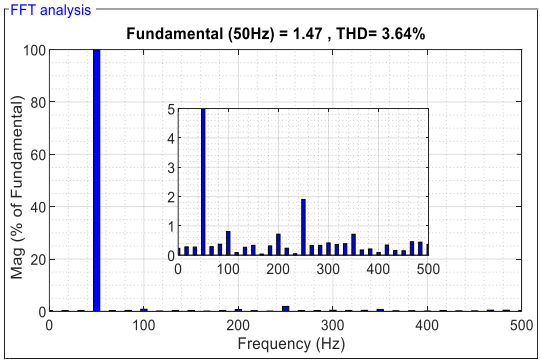

(d) Current THD (FOC-NMSA)

Fig. 10. Second test results.

The values and minimization ratios for each of the undulations, undershoot, SSE, RT, and overshoot for the second test are shown in Table 4. From this table, it is noted that the FOC- NMSTA gave much better values than the FOC-PI and this is shown by the calculated reduction percentages. Accordingly, the FOC-NMSTA reduced the values of response time, SSE, overshoot, ripples, and undershoot of flux by ratios estimated at 40.29 %, 30 %, 77.82 %, 87.76 %, and 86.29 %, respectively. Also, the values of RT, overshoot, ripples, and undershoot torque were reduced by ratios estimated at 52.77 %, 62.79 %, 72.41 %, and 55.55 %, respectively, compared to the FOC-PI. In the case of speed, the FOC-NMSTA reduced the values of RT, SSE, overshoot, and undershoot by ratios estimated at 10.44 %, 66.07 %, 89.92 %, and 95.05 %, respectively, compared to the FOC-PI. Therefore, the FOC-NMSTA has high competence, and this appears through the high reduction rates.

Table 4. Numerical results in the Test 2

	Techniques	w_r(rad/sec)	Q_r(wb)	T_e (N.m)
RT	**FOC-PI**	00.67	00.67	0.36
	FOC-NMSTA	0.06	0.04	0.17
	Ratios (%)	10.44	40.29	52.77
SSE	**FOC-PI**	0.056	0.12	-
	FOC-NMSTA	00.19	0.084	-
	Ratios (%)	66.07	30	-
Overshoot	**FOC-PI**	1.29	0.046	0.86
	FOC-NMSTA	0.13	0.0102	0.32
	Ratios (%)	89.92	77.82	62.79
Ripples	**FOC-PI**	-	0.076	0.58
	FOC-NMSTA	-	00.093	0.16
	Ratios (%)	-	87.76	72.41
Undershoot	**FOC-PI**	1.65	0.054	0.36
	FOC-NMSTA	00.81	0.0074	0.16
	Ratios (%)	95.09	86.29	55.55

c) Third test: Variation of the stator resistance

This test differs from other tests, as the stator resistance value is changed according to Figure 11a to study the extent to which the competence of the FOC-NMSTA is affected compared to the FOC-PI. In this test, the reference speed is made to take a constant value of 157 rad/s, and a load of 4 N.m is applied at the moment for 1.5 s.

Figures 11b and 11c represent the torque and speed for the two controls, where the speed and torque follow the orientation values well, with the FOC-NMSTA having an advantage in terms of RT and undulations compared to the FOC-PI.

The speed in the case of applying FOC-NMSTA is not affected by the change in torque compared to the speed in the case of the FOC-PI.

In Figures 11d and 11e, the flux and current for the two controls are represented, where the value of the stream is connected to the torque and its change. When the load torque is applied, a noticeable increase in the current value is observed for the two controls, with FOC-NMSTA having an improvement in terms of current undulations compared to the FOC-PI. Also, the current remains sinusoidal. The value of the stream fluctuations was 0.206 A and 0.103 A for both the FOC-PI and the FOC-NMSTA, respectively. So the FOC-NMSTA minimized stream undulations by an estimated 50% compared to the FOC-PI.

The flux for both controls follows the reference well, except exceeding the reference value when using the FOC-PI.

Also, when a load torque is applied, it is observed that the flux is affected in the case of using the FOC-PI with this flux, unlike the FOC-NMSTA, there is no effect or exceeding the limit value, which gives it an advantage.

The THD for the two controls is represented in Figures 11f and 11g, where its value was 0.60 % and 3.68 % for both the FOC-NMSTA and FOC-PI, respectively. So the FOC-NMSTA minimized the THD compared to the FOC-PI, as this reduction was estimated at 83.69 %. Also, the amplitude of the FS (50 Hz) was 1.467 % and 1.47 % for both the FOC-NMSTA and FOC-PI, respectively. So, the FOC-NMSTA provided a lower amplitude than the amplitude offered by the FOC-PI. This negativity can be attributed to the values of the NMSTA controller parameters, as this negativity can be defeated in the future using genetic algorithms.

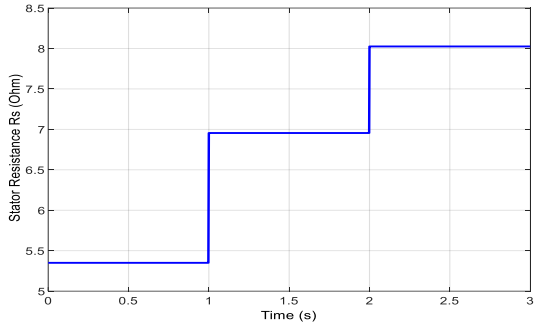

(a) Variation stator resistance

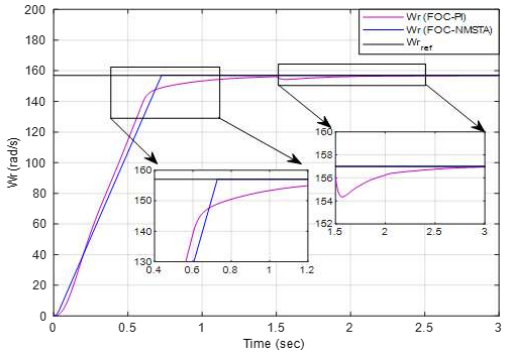

(b) Rotor speed

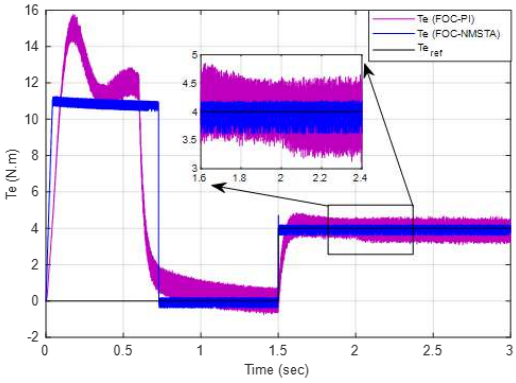

(c) Torque

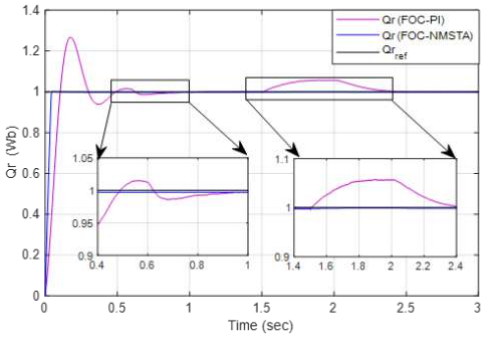

(d) Rotor flux

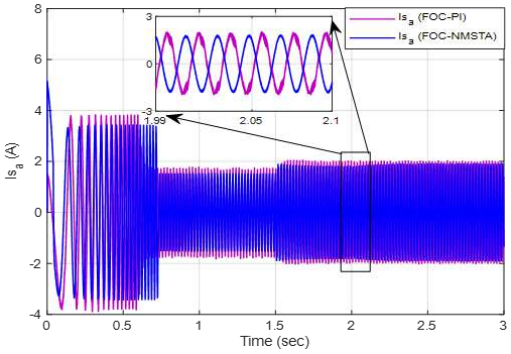

(e) Current

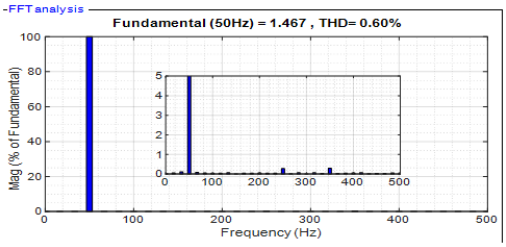

(f) Current THD (FOC-PI)

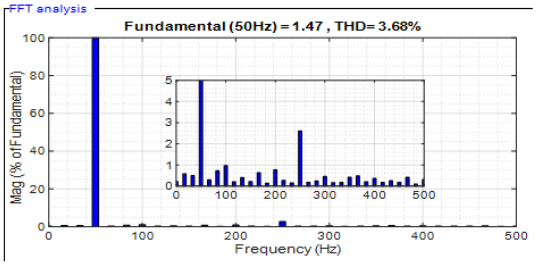

(g) Current THD (FOC-NMSA).

Fig. 11. Third test results.

The numerical values for test 3 are listed in Table 5, where the necessary minimization ratios were determined. Through this table, the FOC-NMSTA minimized the RT compared to the FOC-PI by ratios estimated at 10.44 %, 40.29 %, and 52.77 % for speed, flux, and torque, respectively. Also, the FOC-NMSTA reduced the SSE value for both flux and speed compared to the FOC-PI, where the minimization percentages were estimated at 39.39 % and 70 % for both speed and flux, respectively. Both flux and torque undulations were

minimized by rates estimated at 82.22 % and 55.26 %, respectively, compared to the FOC-PI. Also, the FOC-NMSTA minimized the undershoot value speed, flux, and torque having ratios estimated at 97.38 %, 92 %, and 81.08 %, respectively, compared to the FOC-PI. The overshoot values for speed, flux, and torque were also minimized compared to the FOC-PI, as this minimization was estimated at 95.56 %, 57.24 %, and 41.02 %, respectively. So the FOC-NMSTA has a high competence in this test, and this is shown by the determined minimization rates.

Table 5. Numerical results in the Test 3

	Techniques	w_r(rad/sec)	Q_r(Wb)	T_e (N.m)
RT	**FOC-PI**	00.67	00.67	0.36
	FOC-NMSTA	0.06	0.04	0.17
	Ratios (%)	10.44	40.29	52.77
SSE	**FOC-PI**	0.033	00.8	-
	FOC-NMSTA	00.2	00.24	-
	Ratios (%)	39.39	70	-
Overshoot	**FOC-PI**	0.65	0.028	0.78
	FOC-NMSTA	0.028	0.012	0.46
	Ratios (%)	95.56	57.14	41.02
Ripples	**FOC-PI**	-	0.0045	0.38
	FOC-NMSTA	-	0.0008	0.17
	Ratios (%)	-	82.22	55.26
Undershoot	**FOC-PI**	1.3	0.08	0.46
	FOC-NMSTA	0.034	0.0064	0.087
	Ratios (%)	97.38	92	81.08

d) Fourth test: Change the direction of rotation of the speed

This test aims to study the effectiveness of FOC-MSTA in the case of changing the direction of rotational speed compared to the FOC-PI, where the speed is changed from 157 rad/s to -80 rad/s. The test results are shown in Figure 12. It is noted that the torque, flux, and speed follow the references well, with the FOC-NMSTA having an advantage in terms of RT, overshoot, and undulations compared to the FOC-PI. The FOC-NMSTA did not exceed the limit value for both flux and speed, which gives it an advantage and proves its high performance. The stream for the two controls is shown in Figure 12d, where the value of the current remains related to the system and the torque changes. The value of the current is affected by a change in the direction of the rotation speed, as it is observed at the moment of 1.5 seconds that the value of the current increases while remaining in a sinusoidal shape. The value of the current ripples was 0.39 A and 0.025 A for both the FOC-PI and the FOC-NMSTA, respectively. So, the FOC-NMSTA minimized the current ripples by an estimated rate of 93.58 %, which indicates that the current fineness is high if the FOC-NMSTA is used, which is desirable.

The current THD is present in Figures 12f and 12e for the FOC-NMSTA and FOC-PI methods, respectively. The THD is 4.03 % for the FOC-PI method and 0.89 % for the FOC-NMSTA technique. So the proposed FOC-NMSTA minimized the THD by about 77.91 % compared to the PI-FOC. Also, the two controls provided the same amplitude for the FS (50 Hz), as the value of this capacity was estimated at 1.467 A.

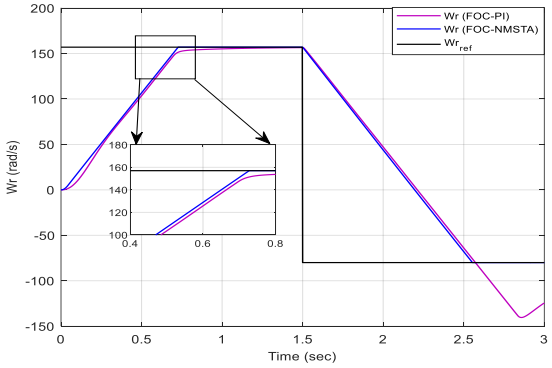

(a) Speed

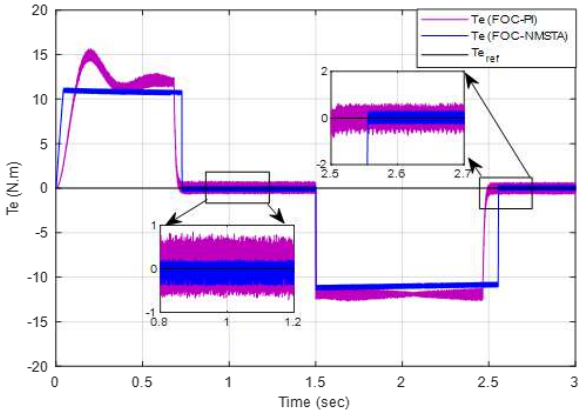

(b) Torque

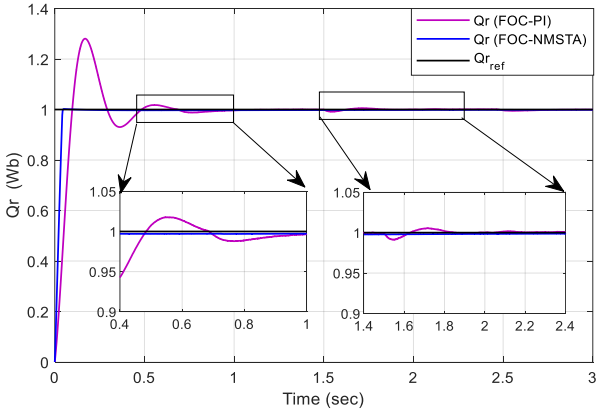

(c) Rotor flux

Table 6 shows that the FOC-NMSTA has better numerical values than the PI-FOC in the fourth test. The proposed FOC-NMSTA minimized the undulations in the flux and torque

compared to traditional FOC with PI controllers. The torque undulations are 0.55 N.m for the FOC-PI and 0.14

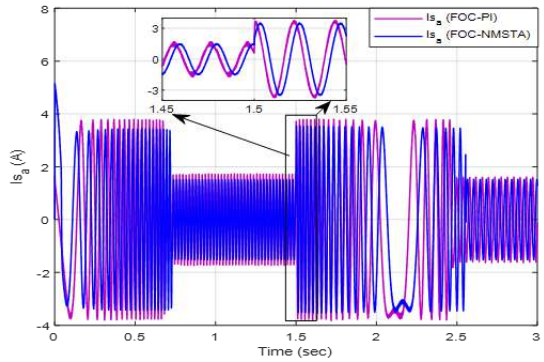

(d) Current

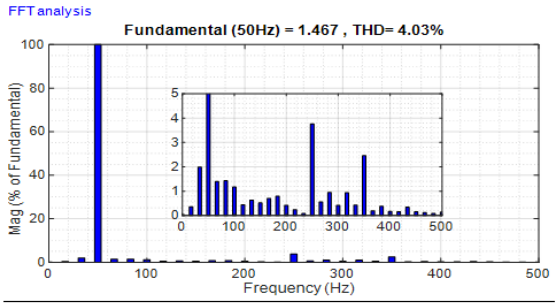

(e) Current THD (FOC-PI)

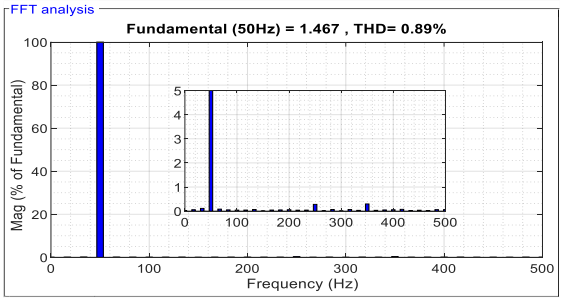

(f) Current THD (FOC-NMSA)

Fig. 12. Fourth test results.

N.m for the designed FOC-NMSTA approach. So, the FOC-NMSTA minimized the torque ripples by about 74.54 % compared to the PI-FOC. The FOC-NMSTA also reduced flux ripples by an estimated 86 % compared to the FOC-PI.

The RT for speed, flux, and torque is better when using the FOC-NMSTA compared to the FOC- PI. The response time minimization was estimated at 10.44 %, 40.29 %, and 52.77 % for speed, flux, and torque, respectively.

The FOC-NMSTA reduced the value of both overshoot and undershoots for flux, speed, and torque compared to the FOC-PI. Accordingly, the FOC-NMSTA minimized overshoot by percentages estimated at 64.56 %, 73.50 %, and 44 % for speed, flux, and torque, respectively. Also, undershooting was reduced by 99.81 %, 75 %, and 73.07 % for speed, flux, and torque, respectively. These relatively high ratios prove the high efficiency of the FOC-NMSTA in this test.

Table 6. Numerical results in the Test 4

	Techniques	w_r(rad/sec)	Q_r(Wb)	T_e (N.m)
RT	**FOC-PI**	00.67	00.67	0.36
	FOC-NMSTA	0.06	0.04	0.17
	Ratios (%)	10.44	40.29	52.77
SSE	**FOC-PI**	0.052	00.71	-
	FOC-NMSTA	0.02	0.39	-
	Ratios (%)	61.53%	45.07%	-
Overshoot	**FOC-PI**	1.27	0.02	0.75
	FOC-NMSTA	0.45	0.053	0.42
	Ratios (%)	64.56	73.5	44
Ripples	**FOC-PI**	-	0.005	0.55
	FOC-NMSTA	-	0.007	0.14
	Ratios (%)	-	86	74.54
Undershoot	**FOC-PI**	1.8	0.02	0.26
	FOC-NMSTA	0.034	0.05	0.07
	Ratios (%)	99.81	75	73.07

In Table 7, the change in the THD for the two approaches in the tests is studied compared to the first test. Through this completed study, it is noted that the THD changed in all tests for the two controls, as its value increased from one test to another. The THD value of FOC-PI was estimated to change in ratios of 6.04 %, 7.06 %, and 15.13% for test 2-test 1, test 3-test 1, and test 4-test 1, respectively. It is noted that this percentage of change is increasing, which indicates that the THD in Test 4 has changed a lot. The same observations are made for the FOC- NMSTA. It is noted that the THD has changed a lot from one test to another, as in Test 4 the value was much greater than the THD in the first test. Therefore, the percentages of change for THD in the case of the FOC-NMSTA were 15.78 %, 20 %, and 46.06 % for test 2 -test 1, test 3 - test 1, and test 4 - test 1, respectively. From the ratios presented, it is noted that the FOC- NMSTA provided greater ratios of change compared to the FOC-PI, where the largest ratio was 46.06 % in the case of using the FOC-NMSTA (test 4 - test 1).

Table 7. Study of the change in the THD for the both controls.

	THD (%)	
	FOC-PI	**FOC-NMSA**
Test_1	3.42	0.48
Test_2	3.64	0.57
Test_2 - Test_1	0.22	0.09
Ratios (%)	6.04	15.78
Test_3	3.68	0.60
Test_3 - Test_1	0.26	0.12
Ratios (%)	7.06	20
Test_4	4.03	0.89
Test_4 - Test_1	0.61	0.41
Ratios (%)	15.13	46.06

In Table 8, the advantage of the FOC-NMSTA technique over some existing approaches is highlighted in terms of the current THD value. This table highlights that the FOC-NMSTA gave a value for THD that is much lower than several nonlinear approaches such as SC and hybrid strategies such as fuzzy DTC, which makes this FOC-NMSTA technique a promising solution for controlling machines in the future.

Table 8. Comparison with other papers in terms of the stream THD values

References	Controls		THD (%)
[58]	SC		11.80
[48]	Parallel PI-based FOC		1.86
[59]	7-level DTC		26.92
	7-level NN-DTC		12.29
[15]	Third-order SMC-based BC		1.09
[60]	Predictive DTC		13.4
[44]	Test 1	DTC	27.03
		NN-DTC	18.49
	Test 2	DTC	40
		N-DTC	32.14
	Test 3	DTC	40
		NN-DTC	18.44
[45]	FOC based on SC-STAs		0.51
[61]	DTC		11.86
	Fuzzy DTC		7.51
[62]	DTC		7.98
	Ant colony algorithm-based DTC		4.82
FOC-NMSTA	Test_1		0.48
	Test_2		0.57
	Test_3		0.60
	Test_4		0.89

6. Conclusions

In this study, a new control called FOC-NMSTA was presented and tested for AM operation. This designed control relies on using the PWM to control the inverter, which makes it simple and uncomplicated. This designed technique was compared with the FOC-PI, where MATLAB was used for this purpose under diverse working conditions, such as changing the direction of rotation and changing the value of the Rs. The most prominent conclusions and performances of FOC-NMSTA can be summarized in the following points:

- Reducing the THD value compared to FOC-PI (by percentages estimated at 85.96 %, 84.34 %, 83.69 %, and 77.91 % in the tests performed)
- Improving the DR of torque, speed, and flux compared to FOC-PI
- Increasing the robustness of the proposed control system
- Improving the SSE value of both flux and speed
- Improved undershoot/overshoot value of speed, flux, and torque compared to FOC-PI

In future work, the FOC-NMSTA approach will be experimentally tested using dSPACE 1104 and compared with other strategies. A genetic algorithm will be proposed to calculate the control parameters. Furthermore, the proposed approach could be combined with other strategies, such as fractional calculus, to further enhance performance and efficiency.

References

[1] Z. Li, Y. Du, J. Ji, T. Tao and W. Zhao, “Zero-sequence Current Suppressing Strategy for Dual Three-phase Permanent Magnet Synchronous Machines Connected with Single Neutral Point”, in CES Transactions on Electrical Machines and Systems, vol. 6, no. 4, pp. 465-472, December 2022. Doi: 10.30941/CESTEMS.2022.00058.

[2] F. Farokhi, N. Wu, D. Smith and M. A. Kaafar, “The Cost of Privacy in Asynchronous Differentially-Private Machine Learning”, in IEEE Transactions on Information Forensics and Security, vol. 16, pp. 2118-2129, 2021. Doi: 10.1109/TIFS.2021.3050603.

[3] Arias, J. Caum, E. Ibarra and R. Griñó, “Reducing the Cogging Torque Effects in Hybrid Stepper Machines by Means of Resonant Controllers”, in IEEE Transactions on Industrial Electronics, vol. 66, no. 4, pp. 2603-2612, April 2019. Doi: 10.1109/TIE.2018.2844786.

[4] N. Zhi, X. Ming, Y. Ding, L. Du and H. Zhang, “Power-Loop-Free Virtual DC Machine Control With Differential Compensation”, in IEEE Transactions on Industry Applications, vol. 58, no. 1, pp. 413-422, Jan.-Feb. 2022. Doi: 10.1109/TIA.2021.3119512.

[5] Y. Shen and Z. Q. Zhu, “Analysis of Electromagnetic Performance of Halbach PM Brushless Machines Having Mixed Grade and Unequal Height of Magnets”, in IEEE Transactions on Magnetics, vol. 49, no. 4, pp. 1461-1469, April 2013. Doi: 10.1109/TMAG.2012.2227147

[6] Y. Chen and V. Dinavahi, “Digital Hardware Emulation of Universal Machine and Universal Line Models for Real-Time Electromagnetic Transient Simulation”, in IEEE Transactions on Industrial Electronics, vol. 59, no. 2, pp. 1300-1309, Feb. 2012. Doi: 10.1109/TIE.2011.2157296.

[7] Fatemi and D. Lahr, “A Comparative Study of Cycloidal Reluctance Machine and Switched Reluctance Machine”, in IEEE Transactions on Energy Conversion, vol. 36, no. 3, pp. 1852-1860, Sept. 2021. Doi: 10.1109/TEC.2021.3050344.

[8] L. Liyi et al., “Fields and Inductances of the Sectioned Permanent-Magnet Synchronous Linear Machine Used in the EMALS”, in IEEE Transactions on Plasma Science, vol. 39, no. 1, pp. 87-93, Jan. 2011. Doi: 10.1109/TPS.2010.2051044.

[9] E. Idrissi et al., “Stator Imbalance Defects Diagnosis of Induction Machine Using Thermography and Machine

Learning Algorithms", in IEEE Access, vol. 12, pp. 51606- 51618, 2024. Doi: 10.1109/ACCESS.2024.3382118.

[10] J. Zou, W. Xu and C. Ye, "Improved Deadbeat Control Strategy for Linear Induction Machine", in IEEE Transactions on Magnetics, vol. 53, no. 6, pp. 1-4, June 2017, Art no. 8106804. Doi: 10.1109/TMAG.2017.2675918.

[11] H. Benbouhenni, Z. Boudjema, A. Belaidi, "DFIG-based WT system using FPWM inverter", International Journal of Smart Grid, vol. 2, No. 3, pp. 142-154, 2018.

[12] B. Habib, "Five-level DTC based on ANN of IM using 13-level hysteresis control to reduce torque ripple comparing with conventional control", Acta Technica Corviniensis- Bulletin of Engineering, Vol. 11, No. 2, pp. 55-58, 2018.

[13] M. Elgbaily, F. Anayi, and M. M. Alshbib, "A Combined Control Scheme of Direct Torque Control and Field-Oriented Control Algorithms for Three-Phase Induction Motor: Experimental Validation", Mathematics, vol. 10, no. 20, 2022. Doi: 10.3390/math10203842.

[14] B. Çavuş and M. Aktaş, "A New Adaptive Terminal Sliding Mode Speed Control in Flux Weakening Region for DTC Controlled Induction Motor Drive", in IEEE Transactions on Power Electronics, vol. 39, no. 1, pp. 449-458, Jan. 2024. Doi: 10.1109/TPEL.2023.3326383.

[15] D. Zellouma, H. Benbouhenni, Y. Bekakra, "Backstepping Control Based on a Third- order Sliding Mode Controller to Regulate the Torque and Flux of Asynchronous Motor Drive", Periodica Polytechnica Electrical Engineering and Computer Science, vol. 6, No. 01, pp. 10-20, 2022. https://doi.org/10.3311/PPee.20333.

[16] K. Szabat, T. Orlowska-Kowalska and M. Dybkowski, "Indirect Adaptive Control of Induction Motor Drive System With an Elastic Coupling", in IEEE Transactions on Industrial Electronics, vol. 56, no. 10, pp. 4038-4042, Oct. 2009. Doi: 10.1109/TIE.2009.2022514.

[17] M. M. Ali, W. Xu, A. K. Junejo, M. F. Elmorshedy and Y. Tang, "One New Super- Twisting Sliding Mode Direct Thrust Control for Linear Induction Machine Based on Linear Metro", in IEEE Transactions on Power Electronics, vol. 37, no. 1, pp. 795-805, Jan. 2022. Doi: 10.1109/TPEL.2021.3096066.

[18] B. Habib, "Rotor flux and torque ripples minimization for direct torque control of DFIG by NSTSM algorithm", Majlesi Journal of Energy Management, Vol. 7, No. 3, 2018.

[19] B. Habib, Z. Boudjema, A. Belaidi, "Direct power control with NSTSM algorithm for DFIG using SVPWM technique", Iranian Journal of Electrical & Electronic Engineering, vol. 17, No. 1, pp. 1-11, 2021.

[20] B. Habib, H. Gasmi, "Comparative Study of Synergetic Controller with Super Twisting Algorithm for Rotor Side Inverter of DFIG", International Journal of Smart Grid-ijSmartGrid, vol. 6, No 4, pp. 144-156, 2022. https://doi.org/10.20508/ijsmartgrid.v6i4. 265.g228.

[21] N. Debdouche, L. Zarour, A. Chebabhi, N. Bessous, B. Habib, I. Colak, "Genetic algorithm-super-twisting technique for grid-connected PV system associate with filter", Energy Reports, vol. 10, pp. 4231-4252, 2023. https://doi.org/10.1016/j.egyr.2023.10.074.

[22] B. Habib, "A Novel Direct Active and Reactive Power Control Method Using Fuzzy Super Twisting Algorithms and Modified Space Vector Modulation Technique for an Asynchronous Generator-based Dual-rotor Wind Powers", Iranian (Iranica) Journal of Energy and Environment, vol.12, No.2, pp. 109-117, 2021.

[23] H. Gasmi, H. Benbouhenni, S. Mendaci, I. Colak, "A new scheme of the fractional-order super twisting algorithm for asynchronous generator-based wind turbine", Energy Reports, vol. 9, pp. 6311-6327, 2023. https://doi.org/10.1016/j.egyr.2023.05.267.

[24] Yahdou, A. B. Djilali, E. Bounadja, B. Habib, "Using neural network super- twisting sliding mode to improve power control of a dual-rotor wind turbine system in normal and unbalanced grid fault modes", International Journal of Circuit Theory and Applications, vol. 0, No. 0, 2024. https://doi.org/10.1002/cta.3960

[25] J. Wang, X. Li, J. Fei, "Evaluation of Interval Type-2 Fuzzy Neural Super-Twisting Control Applied to Single-Phase Active Power Filters", Appl. Sci., vol. 14, pp. 3271, 2024. https://doi.org/10.3390/app14083271.

[26] H. Gasmi, M. Sofiane, H. Benbouhenni, and N. Bizon, "Optimal Operation of Doubly- fed Induction Generator used in a Grid-Connected Wind Power System", Iranian Journal of Electrical and Electronic Engineering vol. 19, No. 2, pp. 2431-2431, 2023. https://doi.org/10.22068/IJEEE.19.2.2431.

[27] M. Ilyas, S. Aziz, I. Shah, A. Khan, D.-W. Jung, "Experimental Stability Analysis of Vertical Takeoff and Landing System Based on Robust Control Strategy", Appl. Sci., vol. 13, pp. 11209, 2023. https://doi.org/10.3390/app132011209

[28] B. Habib, S. Lemdani, "Combining synergetic control and super twisting algorithm to reduce the active power undulations of doubly fed induction generator for dual-rotor wind turbine system", Electrical Engineering & Electromechanics, vol. 2021, No. 3, pp. 8-17, 2021. Doi: https://doi.org/10.20998/2074-272X.2021.3.02.

[29] B. Habib, Z. Boudjema, A. Belaidi, "Comparison study between neural STSM and ANFIS-STSM method in DPC control scheme of DFIG-based dual-rotor wind turbines", International Journal of Mathematics and Computers in Simulation, vol. 14, pp. 73-86, 2020.

[30] B. Habib, N. Bizon, I. Colak, P. Thounthong, N. Takorabet, "Simplified Super Twisting Sliding Mode Approaches of the Double-Powered Induction Generator-Based Multi- Rotor Wind Turbine System",

Sustainability, vol. 14, pp. 5014, 2022. https://doi.org/10.3390/su14095014.

[31] X. Miao, W. Yao, H. Ouyang, Z. Zhu, "Novel Composite Speed Control of Permanent Magnet Synchronous Motor Using Integral Sliding Mode Approach", Mathematics, vol. 11, pp. 4666, 2023. https://doi.org/10.3390/math11224666.

[32] Y. Ye, S. Hu, X. Zhu, Z. Sun, "An Improved Super-Twisting Sliding Mode Composite Control for Quadcopter UAV Formation", Machines, vol. 12, pp. 32, 2024. https://doi.org/10.3390/machines12010032

[33] B. Habib, M. Yessef, I. Colak, N. Bizon, H. Kotb, K. M. AboRas, A. ELrashidi, "Dynamic performance of rotor-side nonlinear control technique for doubly-fed multi-rotor wind energy based on improved super-twisting algorithms under variable wind speed", Sci Rep., vol. 14, pp. 5664, 2024. https://doi.org/10.1038/s41598-024-55271-7.

[34] E. Bounadja, A. Yahdou, A. B. Djilali, H. Benbouhenni, I. Colak, "A Novel Adaptive Third-Order Continuous Super-Twisting Controller of a Five Phase Permanent Magnet Synchronous Wind Generator", Electric Power Components and Systems, vol. 0, No.0, pp. 1–19, 2024 .

[35] B. Habib, "Etude comparative entre la DTC neuronale et la DTC basée sur les régulateurs à hysteresis neuronale de la MAS alimentée par onduleur NPC à cinq niveaux", Revue des Energies Renouvelables, vol. 21, No. 2, pp. 207-216, 2018.

[36] B. Habib, Z. Boudjema, A. Belaidi, "Sensorless twelve sectors implementation of neural DPC controlled DFIG for reactive and active powers ripples reduction", Majlesi Journal of Energy Management, vol. 7, No. 2, 2018.

[37] L. J. Rashad, F. A. Hassan, "Artificial Neural Estimator and Controller for Field Oriented Control of Three-Phase IM", I.J. Intelligent Systems and Applications, vol. 6, pp. 40-48, 2019. DOI: 10.5815/ijisa.2019.06.04.

[38] Z. Boudjema, H. Benbouhenni, A. Bouhani, F. Chabni, "DSPACE implementation of a neural SVPWM technique for a two level voltage source inverter", Iranian Journal of Electrical & Electronic Engineering, vol. 17, No. 3, pp.19-28, 2021.

[39] H. Benbouhenni, I. Colak, N. Bizon, E. Abdelkarim, "Fractional-order neural control of a DFIG supplied by a two-level PWM inverter for dual-rotor wind turbine system", Measurement and Control, vol. 57, No. 3, pp. 1-18, 2023.

[40] B. Habib, N. Bizon, "A new direct power control method of the DFIG-DRWT system using neural PI controllers and four-level neural modified SVM technique", Journal of Applied Research and Technology, vol. 21, No. 1, pp. 36-55, 2023.

[41] B. Habib, M. Yessef, N. Bizon, S. Kadi, B. Bossoufi, A. Alhejji, "Hardware-in- the-loop simulation to validate the fractional-order neuro-fuzzy power control of variable-speed dual-rotor wind turbine systems", Energy Reports, vol. 11, pp. 4904- 4923, 2024. https://doi.org/10.1016/j.egyr.2024.04.049.

[42] H. Benbouhenni, I. Laurentiu-Mihai, M. Alin-Gheorghita, D. Zellouma, I. Colak, N. Bizon, "Active and reactive power vector control using neural-synergetic-super twisting controllers of induction generators for variable-speed contra-rotating wind turbine systems", Measurement and Control, vol. 0, no. 0, 2024. doi:10.1177/00202940231224386.

[43] B. Habib, H. Gasmi, N. Bizon, "Direct Reactive and Active Power Regulation of DFIG using an Intelligent Modified Sliding-Mode Control Approach", International Journal of Smart Grid-ijSmartGrid, vol. 6, No. 4, pp. 157-172, 2022. https://doi.org/10.20508/ijsmartgrid.v6i4.266.g229.

[44] B. Habib, N. Bizon, I. Colak, M. Iliescu, P. Thounthong, "A new direct torque control of an efficient and cost-effective traction system using two squirrel cage induction motors feed by a single inverter", Electric Power Components and Systems, 2024. DOI:10.1080/15325008.2024.2325541.

[45] D. Zellouma, B. Habib, N. Bizon and Y. Bekakra, "A New Field-Oriented Control for Induction Motor Drive Using a Synergetic-Super Twisting Algorithm", 2023 15th International Conference on Electronics, Computers and Artificial Intelligence (ECAI), Bucharest, Romania, 2023, pp. 1-6, doi: 10.1109/ECAI58194.2023.10193989.

[46] Ammar, B. Talbi, T. Ameid, Y. Azzoug, and A. Kerrache, "Predictive direct torque control with reduced ripples for induction motor drive based on T-S fuzzy speed controller", Asian J. Control, vol. 21, no. 4, pp. 2155–2166, 2019. Doi: 10.1002/asjc.2148.

[47] Khaliq et al., "Indirect Vector Control of Linear Induction Motors Using Space Vector Pulse Width Modulation", Comput. Mater. Contin., vol. 74, no. 3, pp. 6263–6287, 2023. Doi: 10.32604/cmc.2023.033027.

[48] D. Zellouma, Y. Bekakra, and B. Habib, "Field-oriented control based on parallel proportional–integral controllers of induction motor drive", Energy Reports, vol. 9, pp. 4846–4860, 2023. Doi: 10.1016/j.egyr.2023.04.008.

[49] V. I. Utkin, D. S. Chen, S. Zarei, and J. Miller, "Sliding mode observers for automotive alternators", Proc. Am. Control Conf., vol. 1, no. June, pp. 165–166, 1999. Doi: 10.1109/acc.1999.782760.

[50] Habib, Z. Boudjema, N. Bizon, P. Thounthong, and N. Takorabet, "Direct Power Control Based on Modified Sliding Mode Controller for a Variable-Speed Multi-Rotor Wind Turbine System Using PWM Strategy", Energies, vol. 15, no. 10, p. 3689, May 2022. Doi: 10.3390/en15103689.

[51] H. Benbouhenni and N. Bizon, "Improved rotor flux and torque control based on the third-order sliding mode scheme applied to the asynchronous generator for the single- rotor wind turbine", Mathematics, vol. 9, no. 18, 2021. Doi: 10.3390/math9182297.

[52] R. Majdoul, A. Touati, A. Ouchatti, A. Taouni, and E. Abdelmounim, "Comparison of backstepping, sliding mode and PID regulators for a voltage inverter", Int. J. Electr. Comput. Eng., vol. 12, no. 1, pp. 166–178, 2022. Doi: 10.11591/ijece.v12i1.pp166-178.

[53] Lascu, A. Argeseanu, and F. Blaabjerg, "Super twisting Sliding-Mode Direct Torque and Flux Control of Induction Machine Drives", IEEE Trans. Power Electron., vol. 35, no. 5, pp. 5057–5065, 2020. Doi: 10.1109/TPEL.2019.2944124.

[54] B. Kelkoul and A. Boumediene, "Stability analysis and study between classical sliding mode control (SMC) and super twisting algorithm (STA) for doubly fed induction generator (DFIG) under wind turbine", Energy, vol. 214, p. 118871, 2021, doi: 10.1016/j.energy.2020.118871.

[55] N. S. Nair, V. B. Anoop, V. A. Arun, J. Chandran, and C. S. Sarathmenon, "Simulation of indirect FOC based 3-phase induction motor drive", International Journal of Advanced Research in Electrical, Electronics and Instrumentation Engineering, vol. 4, no. 1, pp. 240–249, 2015.

[56] K. Zeb, Z. Ali, K. Saleem, W. Uddin, M. A. Javed, N. Christofides, "Indirect field- oriented control of induction motor drive based on adaptive fuzzy logic controller", Electr. Eng., vol.99, pp.803–815, 2016.

[57] Gholipour, M. Ghanbari, E. Alibeiki, and M. Jannati, "Sensorless FOC strategy for current sensor faults in three-phase induction motor drives", J. Oper. Autom. Power Eng., vol. 11, no. 1, pp. 1–10, 2023. Doi: 10.22098/JOAPE.2022.9274.1648.

[58] Davis, Z. M. Salameh, S S., Eaves, "Comparison of a synergetic battery pack drive system to a pulse width modulated AC induction motor drive for an electric vehicle", in IEEE Transactions on Energy Conversion, vol.14, No. 2, pp. 245-250, 1999. Doi: 10.1109/60.766990.

[59] H. Benbouhenni, "Seven-level direct torque control of induction motor based on artificial neural networks with regulation speed using fuzzy PI controller", Iranian Journal of Electrical and Electronic Engineering, vol. 14, No.1, pp. 85-94, 2018.

[60] G. Abad, M. Á. Rodriguez, J. Poza, J. "Two-Level VSC Based Predictive Direct Torque Control of the Doubly Fed Induction Ma-chine With Reduced Torque and Flux Ripples at Low Constant Switching Frequency", IEEE Trans. Power Electron., vol. 23, pp. 1050-1061, 2008.

[61] Saoudi, S. Krim, M. F. Mimouni, "Enhanced Intelligent Closed Loop Direct Torque and Flux Control of Induction Motor for Standalone Photovoltaic Water Pumping System", Energies, vol. 14, pp. 8245, 2021.

[62] S. Mahfoud, A. Derouich, N. El Ouanjli, N. V. Quynh, M. A. Mossa, "A new hybrid ant colony optimization based PID of the direct torque control for a doubly fed induction motor", World Electr. Veh. J., vol. 13, pp. 78, 2022.